Indian Journal of Radio & Space Physics
Vol. 17, December 1988, pp. 220-231

One- and Two-Dimensional Models for Middle Atmospheric Minor Constituents

T S N SOMAYAJI & T ARUNAMANI

Physics Department, Andhra University, Visakhapatnam 530 003

The salient features of formulation of one- and two-dimensional models are briefly reviewed. The details of a one-dimensional model developed and the results obtained from this model are presented and discussed. The results obtained from different two-dimensional models are also discussed.

1 Introduction

The minor neutral constituents of the stratosphere play an important role in atmospheric phenomena in the upper atmosphere. For instance, ozone, which has a total content of only 30 ppmv of the atmosphere, is a key constituent that provides the principal heat energy to the stratosphere by strongly absorbing the solar ultraviolet radiation in the wavelength range 200-310 nm. The minor constituents are also important for the ion-chemistry of the D- and E-regions of the ionosphere. The variations of atomic oxygen and nitric oxide cause changes in electron density distribution in this region of the atmosphere. The chemical reactions that determine the neutral composition have longer time constants, when compared to the ion-chemical reactions, and therefore, the variations in the ionization composition of the D- and E-regions are mainly determined by the variations in the neutral composition.

The chemically active minor constituents are produced in the upper atmosphere from the interaction of the solar radiation with the atmosphere. The products of these photochemical reactions are usually highly active and give rise to a variety of chemical reactions in the upper atmosphere, leading eventually to an equilibrium distribution of these minor constituents themselves.

The distribution of the radiatively active minor constituents, viz. O_3, CH_4, H_2O etc., determines the absorption of radiation and the radiation balance at any altitude in the atmosphere. Thus, the minor constituents determine the thermal structure of the atmosphere and the consequent stability, mainly with respect to vertical motions of the atmosphere. The distributions of certain minor constituents which have sufficiently long chemical lifetimes will be influenced by the dynamical processes caused mainly by the thermal structure of the atmosphere. As a consequence of such variations in certain minor constituents, the radiation balance, and hence the thermal state at any given height, might be altered. The chemical processes are also affected through the temperature-dependent reactions.

It is easy to visualize that all the three main atmospheric processes, viz. radiative, chemical and dynamical processes that determine the distribution of the minor constituents in the atmosphere, are strongly coupled with one another through the minor constituents themselves. Thus we have, in the upper atmosphere, a complex photochemical system that is mainly driven by the solar radiation and is subjected to dynamical processes.

Ever since the anthropogenic influence on the atmospheric ozone was suggested by Crutzen[1], Johnston[2] and Molina and Rowland[3], interest has been growing in estimating the short- and long-term variations of atmospheric ozone that can be caused by prescribed scenarios of natural and anthropogenic emissions of oxides of nitrogen and chlorine, by simulation studies. It will be obvious that the atmosphere cannot be simulated in the laboratory. Also, it is extremely difficult to make such measurements which can help to understand these atmospheric processes in detail. Numerical simulation studies are, therefore, necessary. These studies involve the construction of models, which take into account all the known physical and chemical processes. These models can then be used to calculate the composition of the present day atmosphere. These calculations can be checked against observations on the present day atmosphere. The models, thus validated, can be used to calculate the short-and long-term variations in the composition of the atmosphere that can arise from a prescribed scenario of changes in inputs to the atmosphere, such as radiation flux, emission of pollutants into the atmosphere, etc.

Ideally, one has to construct and use three-dimensional models for simulation studies of the type mentioned above. But, these are not yet attempted in any significant measure. One- and two-dimensional models have been developed and used somewhat extensively. The purpose of this paper is to make a brief review of the one- and two-dimensional models of the atmospheric minor constituents, and of the results obtained from these models.

2 Model Formulation

The temporal variation in the number density, n_i, of the ith species in a given volume element of the atmosphere, is given by

$$\partial n_i/\partial t = P_i - L_i - \nabla.\phi_i \qquad \ldots(1)$$

where the first two terms on the R.H.S. of Eq. (1) represent the production and loss from all sources and sinks, and the last term represents the net transport of the ith species. All models use Eq. (1) to determine the distributions of the different atmospheric species, but differ in the formulation of the different terms.

The production and loss terms are evaluated, considering all the relevant chemical and photochemical processes. However, on considerations of computational fastness and economy, certain chemical reactions that are considerably less important in an altitude range and time under consideration, can be neglected in the evaluation of the production and loss terms. One-dimensional (1-D) models which are computationally much faster as compared to the two-dimensional models, can generally use more comprehensive chemical schemes for the evaluation of the production and loss terms. Recently, there has been a tendency to use more comprehensive chemical schemes in 2-D models as well.

A complete discussion of the physical and chemical processes that have to be considered for the evaluation of the chemical and transport terms in Eq: (1) is beyond the scope of this paper. However, for the sake of completeness, we will briefly discuss, in the following sections, the salient features of photochemistry and transport processes that are relevant for modelling.

2.1 Photochemistry

The first quantitative theory of upper atmospheric photochemistry was developed by Chapman[4], mainly to explain the observed ozone distribution, and it considered a pure oxygen atmosphere interacting with the solar ultraviolet radiation. This simple photochemical theory of Chapman, complemented in the succeeding years with considerations of transport only, was reasonably successful in determining the gross features of the odd oxygen distribution in the upper atmosphere. However, after careful determination of the rate constants of some of the reactions, it became clear that it is necessary to consider additional loss mechanisms for ozone. Bates and Nicolet[5] proposed a catalytic loss for ozone in the mesosphere by the hydroxyl radical (OH). Hunt[6] calculated ozone distribution in an oxygen-hydrogen atmosphere including catalytic loss reactions for ozone by the hydrogen oxides, OH and HO_2. Laboratory measurements subsequent to the work of Hunt[6] showed that the actual reaction rate, for the reaction of HO_2 with O_3, is about an order of magnitude smaller than the one that was used by Hunt in his calculations. It was, therefore, recognized that catalytic reactions by the oxides of hydrogen, although important, cannot completely explain the observed ozone distribution. Crutzen[1] proposed that the oxides of nitrogen are important for the ozone budget and hence the photochemistry of the upper atmosphere. Model studies incorporating the catalytic reactions involving the oxides of nitrogen showed that volume mixing ratios of NO_x($NO + NO_2$) of 1 to 10 ppbv, at altitudes 10-40 km are necessary for explaining the observed ozone distribution below 40 km. Measurements of NO_2 by Ackerman and Muller[7] and of NO by Ackerman *et al.*[8] confirmed the existence of these gases in the required concentrations at stratospheric heights. In the last decade or so, interest has also been focussed on the importance of certain chlorine compounds, especially the chlorofluorocarbons, at stratospheric heights. These gases have long residence time in the troposphere, are insoluble in water and are relatively less reactive, and therefore, can slowly be transported into the stratosphere. In the stratosphere, they are photodecomposed by the solar UV radiation, and atomic chlorine (Cl) is released. This atomic chlorine combines with ozone to form chlorine oxide (ClO) and molecular oxygen. The ClO thus formed combines with atomic oxygen to reform atomic chlorine besides molecular oxygen. Thus, the photodissociation products of the chlorine compounds, viz., Cl and ClO participate in a catalytic destruction of odd oxygen in the stratosphere. It is now believed that these catalytic reactions are very important to determine the ozone budget in the stratosphere as pointed out by different workers[3,9-15].

Methane (CH_4) reacts with Cl to form HCl, which has a long chemical lifetime. This particular reaction of CH_4 removes the chemically active chlorine to form a relatively very long lived HCl, thereby dampening the catalytic loss of ozone by Cl and ClO. Methane is mainly lost in the stratosphere through its reaction with OH and subsequent successive oxidation reactions to produce water vapour. However, because of its effect on reducing the catalytic loss of

ozone by the chlorine compounds, reactions involving methane and its oxidation products are also important for stratospheric modelling.

The complete set of chemical and photochemical reactions that need to be considered for modelling the middle atmospheric minor constituents is given by Crutzen *et al.*[16] The necessary data on the reaction rate constants, solar spectral irradiance, photoabsorption cross-sections, etc. were compiled by Deshpande and Mitra[17] and more recently in *WMO report No.* 16 (Ref. 18).

2.2 Solar Radiation

Solar radiation in the wavelength range $100 \text{ nm} < \lambda < 320 \text{ nm}$ and its absorption by the atmosphere is important for the structure of the atmosphere. In the recent past there has been a substantial increase in our knowledge of the 100-320 nm solar spectral irradiance. This has been the result of the recent analyses of data from both the SBUV instruments on the NIMBUS-7 satellite and the SME satellite as reported by different workers[19-26]. The *WMO report No.* 16 (Ref. 18) gives a reference solar spectrum, which is recommended for upper atmospheric modelling.

2.3 Photodissociation Rates

Photodissociation rates for all the compounds with the exception of NO are calculated in the usual way from

$$J(X) = \Sigma\, I_\lambda^\infty \,.\, \sigma_\lambda(X) \,.\, \exp(-\tau) \,.\, d\lambda \qquad \ldots(2)$$

where

I_λ^∞ The flux incident at the top of the atmosphere

$\sigma_\lambda(X)$ The absorption cross-section of the species X at wavelength λ in an interval $d\lambda$

τ The optical depth factor of the radiation at wavelength λ

For calulating the optical depth factor in the above expression, it is assumed that molecular oxygen and ozone are the sole absorbers of radiation. Then the optical depth factor is given by

$$\tau = \left[\sigma_\lambda(O_2) \cdot \int_z^\infty n(O_2) \,.\, dz + \sigma_\lambda(O_3) \times \int_z^\infty n(O_3) \,.\, dz \right] \cdot sec(\chi) \qquad \ldots(3)$$

which can be approximated as

$$\tau = [\sigma_\lambda(O_2) \,.\, n(O_2) \,.\, H(O_2) + \sigma_\lambda(O_3) \,.\, n(O_3) \,.\, H(O_3)] \,.\, \sec(\chi) \qquad \ldots(4)$$

where $\sigma_\lambda(O_2)$ and $\sigma_\lambda(O_3)$ are the absorption cross-sections of O_2 and O_3, respectively, at wavelength λ; $n(O_2)$ and $n(O_3)$ are the concentrations of O_2 and O_3, respectively, at the altitude z; and $H(O_2)$ and $H(O_3)$ are the scale heights of O_2 and O_3, respectively, at the altitude z.

The calculation of the photodissociation rates of NO is somewhat difficult. Absorption of NO occurs in the predissociated bands which overlap the SR bands of O_2. The photodissociation rates of NO are thus dependent on the details of the overlap of these two band systems. Cieslik and Nicolet[27] have made a detailed study of the photodissociation of NO and their estimates of photodissociation coefficients of NO can be adopted for modelling studies.

2.4 The Transport Term

The main difference in 1-D and 2-D models lies in the formulation of the transport term. The 1-D models represent globally averaged altitude distributions and consider transport only in the vertical direction. The transport term in Eq. (1) can then be approximated as

$$\nabla \,.\, \phi_i = \partial \phi_i / \partial z \qquad \ldots(5)$$

where

$$\phi_i = -D_{iN_2}\left[\frac{\partial n_i}{\partial z} + \frac{1}{T}\frac{\partial T}{\partial z} n_i + \frac{n_i}{H_i}\right] - K_z\left[\frac{\partial n_i}{\partial z} + \frac{1}{T}\frac{\partial T}{\partial z} n_i + \frac{n_i}{H_a}\right] \qquad \ldots(6)$$

where D_{iN_2} is the mutual diffusion coefficient between the ith constituent and molecular nitrogen, K_z the vertical eddy diffusion coefficient, T the atmospheric temperature, and H_i and H_a are the scale heights of the ith constituent and the mixed air, respectively.

If one is interested only in the region below the turbopause (say, for example, stratosphere), where the diffusive process is mainly by eddy diffusion, then Eq. (6) can be approximated as

$$\phi_i = -K_z\left[\partial n_i / \partial z + \left(\frac{1}{T}\cdot\frac{\partial T}{\partial z} + \frac{1}{H_a}\right) \,.\, n_i\right] \qquad \ldots(7)$$

which can also be expressed as

$$\phi_i = -K_z \,.\, n(M) \,.\, \partial \mu_i / \partial z \qquad \ldots(8)$$

where $n(M)$ is the air density and μ_i is the volume mixing ratio of the ith constituent.

In the actual model calculations, a set of equations of the type of Eq. (1), wherein the transport term is replaced by using Eqs (5) and (6) or, Eqs (5) and (8), are

written separately for each of the species. The resulting set of equations is solved simultaneously using numerical methods.

2.5 Eddy Diffusion Coefficients

The transport formulation in 1-D models through the use of the eddy diffusion coefficient, K_z, is purely empirical. It does not utilize observed atmospheric motions directly, but is rather based on the observations of the temporal and spatial distributions of selected tracers. The eddy diffusion coefficient is estimated linking it to the mixing length and velocity of turbulent motions which are derived from the observed temporal and spatial variations of tracers[28-30]. Reed and German[31] used published heat flux data to obtain a set of eddy diffusion coefficients for the lower stratosphere. Using the same approach and relating the eddy transport to average fields of meteorological quantities like wind variations and potential temperature, Ebel[32] has developed eddy diffusion models for the upper stratospheric, mesospheric and lower thermospheric heights.

In the treatment of vertical motions through the vertical eddy diffusion coefficient, it is usually assumed that the value of K_z is a function of only motions and remains independent of both the details of the tracer field and the specific structure of tracer sources and sinks. Generally, a single K_z profile is chosen to represent the transport of all the species in the atmosphere. However, it is now recognized that it may not be possible to find a K_z profile that adequately fits atmospheric data for all the long-lived tracers such as N_2O, CH_4 and O_3 at the same time[33]. Using a separate K_z for each species, it would be possible to fit any observational data to the model calculations without necessarily representing any physical aspect of the atmosphere. It looks unreasonable to consider different values of K_z for different species, unless a physically well-defined basis is established for the same. However, some dynamically-based parametrizations have recently been proposed for K_z by Holton[34] and Mahlman *et al.*[35] These treatments, in which K_z depends on the species and their chemical gradients, appear to be promising and need to be fully developed and exploited.

3 One-Dimensional Models

The 1-D models represent the globally and annually averaged atmosphere because all horizontal motions are inherently averaged out by the vertical eddy diffusion representation of transport. Yet, in a sense, these models purport to represent a specific time of the year appropriate to the average solar zenith angle that has been considered in the model calculations.

The 1-D models can be coupled to 1-D radiative models, so that the changes in radiatively active constituents like ozone are fed back to determine changes in temperature structure. The 1-D models with such a feedback can account for global climatic effects resulting from changes in radiatively active trace species.

A feedback which cannot be incorporated into a 1-D model is that due to dynamical changes that occur when variations in radiatively active species, mainly ozone, modify the net heating rate causing changes in transport.

Despite these shortcomings, 1-D models still remain the principal tool to evaluate possible perturbations of minor constituents, mainly ozone, although 2-D models are increasingly being used.

3.1 Computational Technique of a 1-D Model

A time-dependent one-dimensional model for the minor constituents in the mesosphere and lower thermosphere has been developed by us. The details of this model will be published separately. The model calculates the vertical distributions of the odd oxygen (O^3P, O^1D and O_3), the odd hydrogen (H, OH and HO_2) and the odd nitrogen (N, NO and NO_2) in the altitude range 60-120 km at intervals of 2 km. These distributions are determined by obtaining the time-dependent solutions of Eq. (1) in which the transport term is evaluated using Eq. (5), wherein the flux ϕ_i is obtained from Eq. (6). In order to avoid the numerical stiffness problem, a number of photostationary assumptions and a grouping into families of constituents were made. Assuming a set of initial distributions estimated under photostationary conditions and appropriate boundary conditions at the lower and upper boundaries, the set of continuity equations written in their difference form for the three chemical families (the odd oxygen, the odd hydrogen and the odd nitrogen) was solved simultaneously using an integration time step of 1200 s throughout, except for two hours at sunset when a smaller time step of 200 s was used to allow smooth transition from daytime to nighttime conditions. At times when the grouping of the member species into a family is not valid, the family concept is given up and integration carried out independently for the different members of the family.

Integration was carried out until day-to-day repeatability to within one per cent error at all altitudes and for all the modelled species, was obtained. After such a convergence was reached, the model was run for one more day and the results at noon and midnight times were taken as representative mean values for daytime and nighttime conditions, respectively.

A steady-state 1-D model for the stratospheric altitudes (16-60 km) was also worked out by us. This model calculates the distributions of the odd chlorine

(Cl, ClO, $ClONO_2$ and HCl) compounds, in addition to the odd oxygen, odd hydrogen and odd nitrogen species, besides the source gases, viz. N_2O, H_2O, and certain halocarbons and hydrocarbons. The model calculations are made nearly in the same manner as for the mesospheric model described above, but by solving the set of continuity equations simultaneously for steady-state solutions, i.e. by assuming the time variations as zero [$(\partial n_i/\partial t = 0$ in Eq. (1)].

The vertical distributions were determined for a solar zenith angle of 30° and for solar minimum conditions. The daytime distributions of the mesospheric model and the steady-state distributions of the stratospheric model are, therefore, believed to be appropriate for annual mean of noontime values for a low latitude station under solar minimum conditions.

3.2 Mesospheric Model Results and Some Comparisons

The vertical distributions of the odd oxygen species obtained from our time-dependent 1-D model for the mesosphere and the lower thermosphere are shown in Fig. 1. For these calculations the vertical eddy diffusion coefficient distribution is assumed to be that reported by Holton[36]. In addition to these results, we have plotted in Fig. 1, for comparison, the model results for atomic oxygen obtained using a different eddy diffusion coefficient profile; this profile is based on the *K*-models reported by Ebel[32], results for atomic oxygen reported by Solomon[37] (who used similar model calculations but for a latitude of 30°N), and distributions of ozone based on measurements reported earlier by many workers[38-40]. The vertical distribution of the excited molecular oxygen, $O_2(^1\Delta_g)$ calculated assuming photochemical equilibrium with ozone, is also shown in Fig. 1.

The influence of the assumed eddy diffusion coefficient profile on the model-calculated distribution of atomic oxygen is evident from the deviations in curves labelled 9 and 11. The agreement between our model results for ozone and those based on measurements can be considered as reasonable, keeping in view the fact that 1-D model calculations, at best, represent average conditions in the atmosphere, and some disagreement between the model calculations and individual measurements is to be expected.

Calculated concentrations of odd hydrogen species are shown in Fig. 2 along with rocket measurements of the hydroxyl radical by Anderson[41] and results of a similar model calculations of atomic hydrogen reported by Solomon[37] for a latitude of 30°N. Large differences exist between atomic hydrogen concentrations obtained by us and Solomon. The relative concentrations of OH and HO_2 obtained by us are found to be consistent with theory. The agreement between our model calculations for OH and the observations of Anderson is satisfactory.

The model results for the odd nitrogen species are shown in Fig. 3 which also shows the rocket-borne measurements of NO by Meira[42] and Tohmatsu and Iwagami[43]. The agreement between the model results

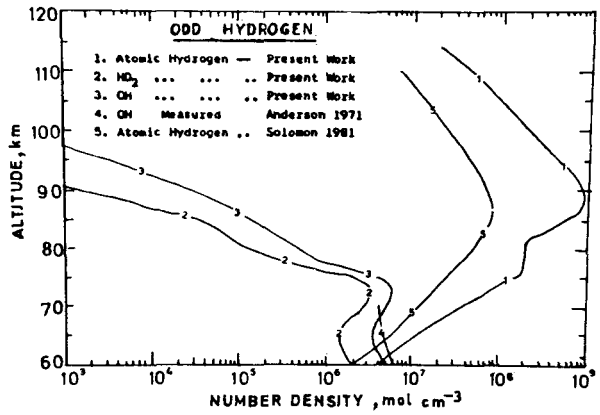

Fig. 2—Altitude distribution of odd hydrogen compounds in the mesosphere

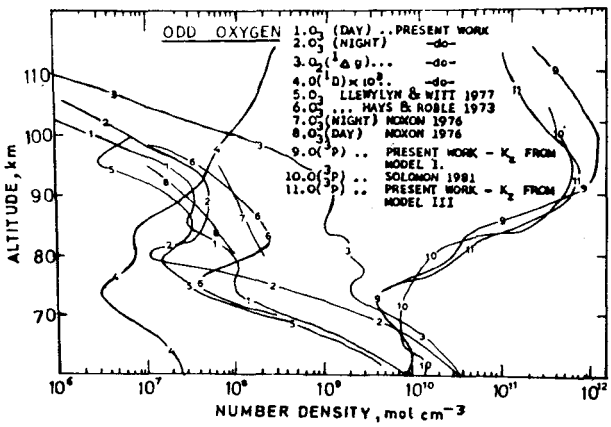

Fig. 1—Altitude distribution of odd oxygen species in the mesosphere

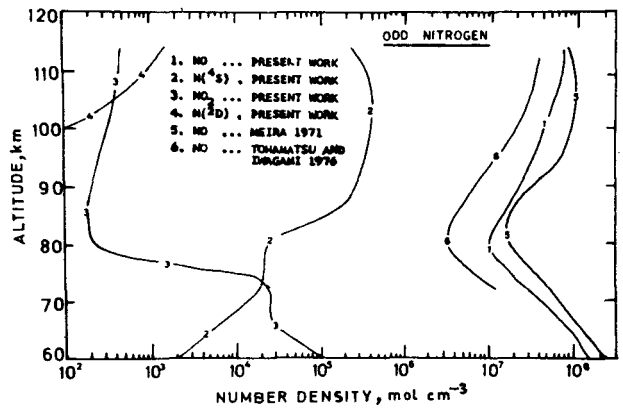

Fig. 3—Altitude disribution of odd nitrogen compounds in the mesosphere

and the measurements can be considered as satisfactory, in view of the known variability of NO.

The day-night variations of model-calculated ozone concentrations at different altitudes are shown in Fig. 4. It is to be noted that at altitudes below 76 km the nighttime concentrations of ozone are higher than the daytime values. This indicates a gradual conversion of atomic oxygen into ozone through the three body reaction, $O + O_2 + M \rightarrow O_3$, at night in the absence of photolysis of O_3.

3.3 Stratospheric Model Results

The altitude distributions of concentrations of odd oxygen (O^3P, O^1D and O_3), odd hydrogen (H, OH, HO_2 and H_2O_2), odd nitrogen (NO, NO_2, HNO_3, N and NO_3) and odd chlorine (Cl, ClO, $ClONO_2$ and HCl) species in the stratosphere (16-60 km) calculated from our steady-state 1-D model are presented and discussed in comparison with similar results reported earlier.

The results for the odd oxygen species are shown in Fig. 5 along with the results of a time-dependent 1-D model calculations reported earlier by Crutzen *et al.*[16], and measurements of ozone made at Thumba by Acharya *et al.*[44] The agreement between the results of our calculations and these earlier results is, in general, satisfactory. Some differences, however, do exist between our results for ozone and the model results of Crutzen *et al.*[16] particularly below the peak of the ozone layer. This is perhaps due to the variation in latitudes considered by the two models (the results of Crutzen *et al.*[16] are for annual mean daytime conditions at 30°N and our results are for a solar zenith angle of 30° which corresponds to an annual mean of noontime conditions at a latitude of 11°N) and also the differences in treatments (Crutzen's model calculates time-dependent solutions while ours calculates for steady-state conditions).

The calculated height distribution of the odd hydrogen species, viz. H, OH, HO_2 and H_2O_2 along with the results of the 1-D model of Crutzen *et al.*[16], are shown in Fig. 6. Also shown in Fig. 6 are the vertical distributions of OH obtained by Solomon and Garcia[45] from a 2-D model, the experimental results of OH deduced from in situ resonance fluorescence measurements by Anderson[46] and Heaps and McGee[47]. The seasonal range of values of OH determined from another 2-D model developed at the Goddard Space Flight Centre, USA, and reported in *WMO report No.* 16 (Ref. 18) is shown as a hatched area in Fig. 6. It can be seen that the agreement among

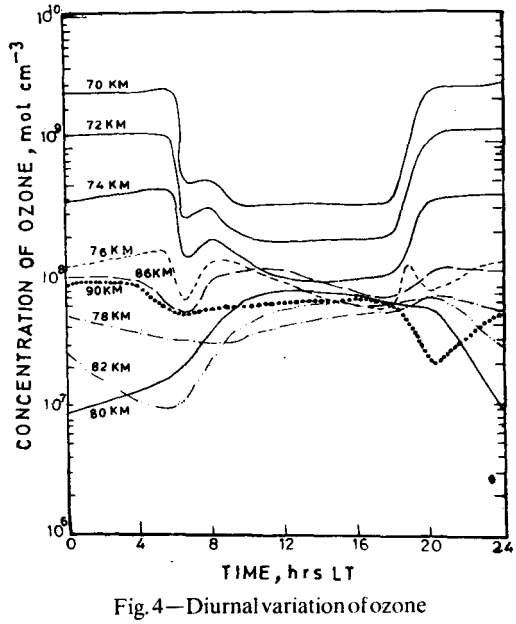

Fig. 4—Diurnal variation of ozone

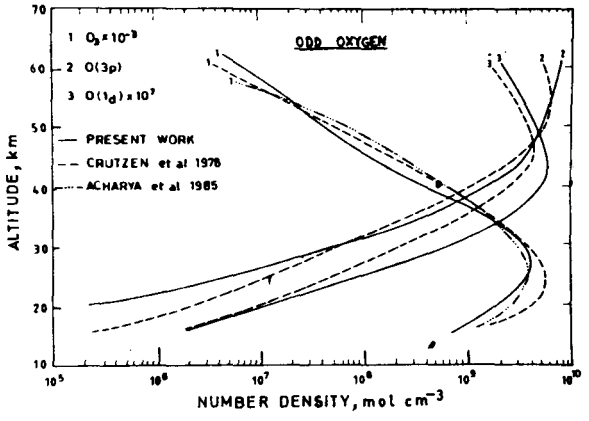

Fig. 5—Altitude distribution of the odd oxygen species in the stratosphere

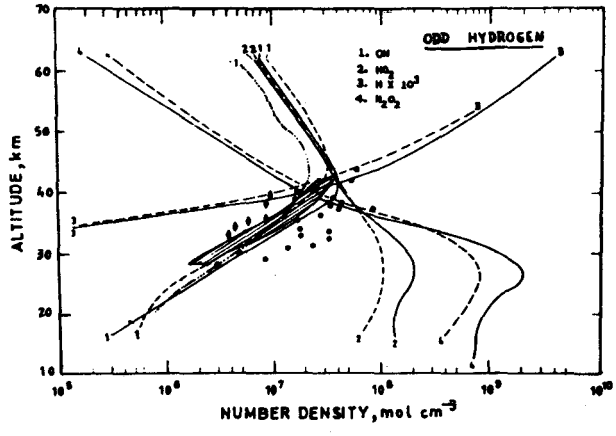

Fig. 6—Altitude distribution of the odd hydrogen species in the stratosphere [—, Present work; – – –, 1-D model results of Crutzen *et al.*[16]; – ··· – ··· –, 2-D model results for OH from Solomon and Garcia[45]; ○○○, In situ resonance fluorescence measurements of OH by Anderson[46]; ◇◇◇, In situ resonance fluorescence measurements of OH by Heaps and McGee[47]; the hatched region is the seasonal range of values of OH determined from a 2-D model of GSFC (USA).]

the results of different model calculations as well as with the experimental results is generally satisfactory.

The model-calculated distribution for odd nitrogen species along with the distribution of the source gas, N_2O, is shown in Fig. 7. Also shown in Fig. 7 are the results of the 1-D model calculations of Crutzen *et al.*[16] Although there is a general agreement between the distributions derived from the two models, deviations, although not excessive, do exist. The deviations in NO are particularly important, because, several chemical reactions that determine the equilibrium concentrations of almost all the minor constituents are sensitively coupled through NO and any error in the model-derived values of NO will cause errors in all the other calculations. It is important to note here that when models are used to assess perturbations to the stratospheric ozone, it is necessary to simulate accurately the response of ozone to changes in oxides of nitrogen. It was found that large differences in model estimates of NO_y($NO + NO_2 + N + NO_3 + HNO_3 + 2 . N_2O_5$.) arise mainly from differences in the treatment of penetration of UV radiation through the SR bands of O_2 (Ref. 18). Because one of the important applications to which both 1-D and 2-D models are put to is to assess perturbations of stratospheric ozone arising from given increases in chlorine compounds there, and because of the strong implication of any error in the model estimates of NO_y on such an assessment, accurate formulation of radiative schemes in the UV is essential for both 1-D and 2-D photochemical models.

For comparison, we have plotted in Fig. 7 the best estimates of NO, NO_2 and HNO_3 made from several measurements using rockets and balloons in the altitude range 16-60 km, at latitudes between 32°N and 40°N, as reported in the *WMO report No.* 16 (Ref. 18). A comparison of these experimental estimates of the oxides of nitrogen with the model results shows only a general agreement with some systematic deviations at all altitudes.

The model results for the distribution of the odd chlorine compounds, viz. Cl, ClO, $ClONO_2$ and HCl along with the 1-D model results of Crutzen *et al.*[16] are shown in Fig. 8. Although there is reasonable agreement, systematic differences do exist. The height region where the chlorine compounds are significant can be seen to be below 45 km. In situ resonance fluorescence measurements of midday ClO were made by Weinstock *et al.*[48] and Brune *et al.*[49] After omitting a few profiles that showed anomalously high mixing ratios, the averages of the above two sets of measurements were reported in the *WMO report No.* 16 (Ref. 18). We plotted these two results also in Fig. 8. The measured values are somewhat higher than the modelled values, particularly, above 30 km. The measurements of $ClONO_2$ made by Murcray *et al.*[50] and Rinsland *et al.*[51] are also shown in Fig. 8. These are consistently higher than the modelled results. It is to be noted that $ClONO_2$ is an important reservoir species, which reduces the efficiency of catalytic destruction of ozone by both the oxides of chlorine and nitrogen.

The height distributions of methane and its oxidation products, determined from our model, are shown in Fig. 9, along with the 1-D model calculations of methane reported by Crutzen *et al.*[16] The model results for the height distribution of the halocarbons, CCl_4, CH_3Cl, $CFCl_3$ and CF_2Cl_2 are shown in Fig. 10 along with the 1-D model results of Crutzen *et al.*[16]

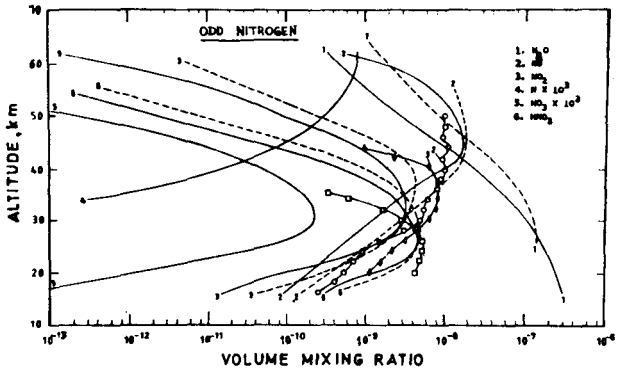

Fig. 7—Altitude distribution of odd nitrogen species and N_2O in the stratosphere [—, Present work; – – –, 1-D model results of Crutzen *et al.*[16]; ◇◇◇, Best estimates of NO_2 at 32°N from non-satellite techniques; ○○○, Best estimates of NO at 32-40°N from all techniques; □□□, Best estimate of HNO_3 at 32°N from several observations]

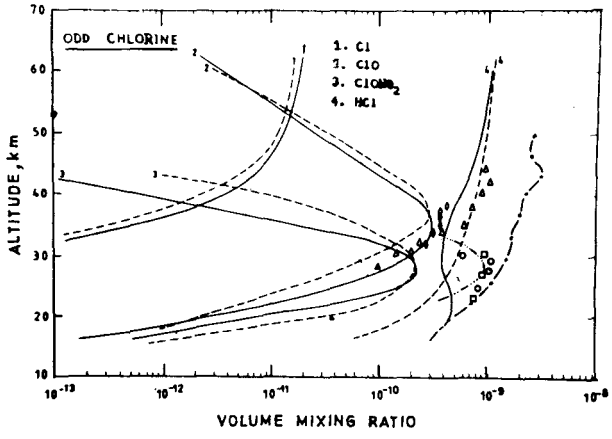

Fig. 8—Altitude distribution of odd chlorine in the stratosphere [—, Present work; – – –, 1-D model results of Crutzen *et al.*[16]; – · – · –, Weighted mean of several measurements of HCl; ◇◇◇, Measurements of ClO by Brune *et al.*[49]; △ △ △, Measurements of ClO by Weinstock *et al.*[48]; – ··· – ···, 2-D model results of $ClONO_2$ from Ko and Sze[73]; ○○○, Measurements of $ClONO_2$ by Rinsland *et al.*[51]; □□□, Measurements of $ClONO_2$ by Murcray *et al.*[50]]

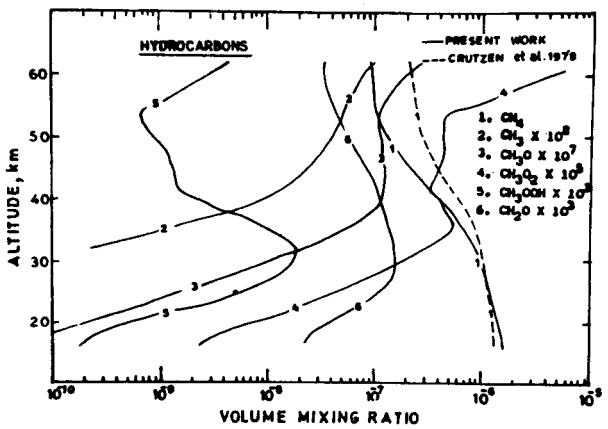

Fig. 9—Altitude distribution of the carbon species in the stratosphere

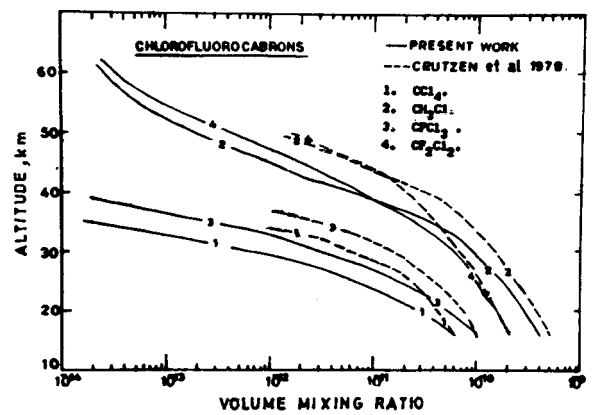

Fig. 10—Altitude distribution of halocarbons in the stratosphere

4 Two-Dimensional Models

As mentioned earlier, the diffusive treatment of the transport in 1-D models is somewhat arbitrary. Further, it is difficult to evaluate accurately the global averages for the production and loss terms in the continuity Eq. (1). Also, latitudinal variation cannot be simulated in a 1-D model. The measured latitudinal distribution of ozone column and some tracers like N_2O indicate the vital role of meridional motions in determining the distributions of these gases. The 2-D models can include this transport, while 1-D models cannot.

Recent model calculations of global depletion of ozone arising from prescribed enhancements in concentrations of chlorine compounds (Cl and ClO) show that 2-D models predict larger values of this quantity than those predicted by the 1-D models. Also, 2-D models predict strong latitudinal gradients of ozone reductions with larger ozone reductions at temperate and polar latitudes than those found by 1-D models. Recently, large scale spring-time depletion of ozone observed at polar zones indicates the advantage of using 2-D models. For certain estimates to be made and for testing certain complex chemistry schemes, 1-D models can, however, be used because of the computational ease.

As mentioned earlier, the main difference between 1-D and 2-D models lies in the formulation of the transport term in the continuity equation [Eq. (1)].

Taking y and z as the meridional and vertical coordinates, the continuity equation for the zonal mean of a tracer gas of volume mixing ratio μ can be written from Eq. (1) as

$$\partial\bar{\mu}/\partial t = P - L - [\bar{v}(\partial\bar{\mu}/\partial y) + \bar{w}(\partial\bar{\mu}/\partial z) + (1/\cos\phi)\,\partial(\overline{v'\mu'}\cos\phi)/\partial y + \{1/n(M)\}\,.\,\partial\{n(M)\,.\,\overline{w'\mu'}\}/\partial z] \quad \ldots(9)$$

where v, w are the meridional and vertical velocity components, $\partial y = a\,.\,\partial\phi$, a being the radius of the earth, ϕ the latitude, $n(M)$ the air density, and P and L are the total production and loss of the species from all sources and sinks. In Eq. (9) the parameters with bars over them represent a zonal average, and parameters with primes represent departures therefrom, and the local value of any parameter is given by the sum of the zonal average and the departures. For example, for the parameter μ, the zonal average is given by

$$(\bar{\mu}) = (1/2\pi)\int_0^{2\pi} (\mu)\,.\,\mathrm{d}\lambda$$

where λ is the longitude. The local value μ is then given by

$$\mu = (\bar{\mu}) + (\mu') \quad \ldots(10)$$

In terms of the parameters with bars and primes, Eq. (9) can be rewritten as

$$\frac{\partial\bar{\mu}}{\partial t} + \bar{v}\cdot\frac{\partial\bar{\mu}}{\partial y} + \bar{w}\frac{\partial\bar{\mu}}{\partial z} = -\frac{1}{\cos\phi}\frac{\partial}{\partial y}(\overline{v'\mu'}\,.\cos\phi) - \frac{1}{n(M)}\frac{\partial}{\partial z}\{n(M)\,.\,\overline{w'\mu'}\} + P - L \quad \ldots(11)$$

In Eq. (11), the transport terms on the left hand side represent advection by a zonal mean circulation and those on the right hand side contain departures from the zonal mean, which are usually referred to as 'eddies'. These eddies arise from wave-type disturbances in the atmosphere. The treatment of these eddies and their proper interpretation are central to the problem of 2-D modelling.

A full discussion of the evolution of 2-D models is beyond the scope of this paper. We briefly present the important phases of 2-D model development, which indicate advances in our understanding of the transport processes and their formulation in a 2-D framework. Further information in this regard can be had from the *WMO report No.* 16 (Ref. 18), and the various references therein.

Prabhakara[52] was the first to model the eddies in a 2-D framework. He considered the eddies as a Fickian diffusion given by

$$\overline{v' . \mu'} = - K_y . \partial\bar{\mu}/\partial y; \quad \overline{w' \mu'} = - K_z . \partial\bar{\mu}/\partial z \qquad \ldots(12)$$

Prabhakara was able to derive the global distribution of ozone that matched observations. But, with the subsequent observation of counter-gradient horizontal fluxes in the lower stratosphere by Newell[53], Prabhakara's treatment of eddies as a Fickian diffusion was questioned, because in a Fickian diffusion (turbulence-type motions)the fluxes must be downgradient only. Motivated to find a solution for this puzzle, Reed and German[31] developed the *K*-theory to include counter-gradient fluxes. Assuming the parcel trajectories to be straight lines inclined to the mean isentropies, Reed and German[31] showed that the fluxes of a quasi-conservative tracer are determined by a symmetric *K*-tensor given by

$$\begin{pmatrix} \overline{v' . \mu'} \\ \overline{w' . \mu'} \end{pmatrix} \equiv - \begin{pmatrix} K_{yy} & K_{yz} \\ K_{yz} & K_{zz} \end{pmatrix} \cdot \begin{pmatrix} \partial\bar{\mu}/\partial y \\ \partial\bar{\mu}/\partial z \end{pmatrix} \qquad \ldots(13)$$

and then the flux would be diffusive.

The thermodynamic and momentum equations have to be solved for the determination of a tracer distribution. These equations contain the respective eddy fluxes, which need to be evaluated first. Heat flux, being a strictly conserved quantity, the eddy heat flux can be calculated using the *K*-tensor given in Eq. (13). Eddy momentum fluxes cannot be calculated using the *K*-tensor, because momentum is not a strictly conserved quantity. To circumvent this problem Rao Vupputuri[54] related the momentum fluxes to the observed vertical wind variations. Using the eddy momentum fluxes, so deduced, the momentum equation was solved. Using satellite data, Harwood and Pyle[55] derived horizontal eddy momentum fluxes, which are used to solve the momentum equation.

Models of the type mentioned above are referred to as classical Eulerian models. These models were successful in providing realistic stratospheric fields of constituent mixing ratios, etc. Subsequently, it has become known that the large-scale atmospheric waves in the middle atmosphere possess coherent structures and do not behave like turbulence[56-59]. Consequently, the assumptions of Reed and German[31] regarding the conservative nature of tracer, the straight line parcel trajectories and the sloping mixing surfaces were all criticized[57,60]. Subsequent analytical studies of transport in the middle atmosphere resulted in a better understanding of the relationship between the mean circulation and eddies and a reassessment of Reed and German's work[31]. Andrews and McIntyre[61] pointed to the desirability of using a Lagrangian procedure, in which averages were taken following the trajectories of air parcels, rather than around fixed latitude circles as is done in the Eulerian formulations. But, because of practical problems of using a Lagrangian procedure[62], alternate Eulerian mean models which retained some of the positive attributes of the Lagrangian mean theory were developed. These are called the transformed Eulerian Models, and can be broadly classified into two types, viz. the residual mean circulation models developed by many workers[57,63-68] and which use pressure as the vertical coordinate; and the formulation in isentropic coordinates developed by Mahlman *et al.*[69] and Tung[70]. The latter models use the potential temperature as the vertical coordinate. Both the formulations have the common feature that for steady and nondissipative small amplitude waves, the mean circulation reduces to the Lagrangian mean circulation.

In the residual mean formulation, the advective transport by the steady adiabatic waves is subtracted from the mean velocities and the residual circulation is defined in terms of two parameters denoted as $\bar{v}_R$ and $\bar{w}_R$, which are given by

$$\bar{v}_R = \bar{v} - \frac{1}{n(M)} \cdot \frac{\partial}{\partial z} \{ n(M) . \overline{v' \theta'} / \bar{\theta}_z \} \qquad \ldots(14)$$

$$\bar{w}_R = \bar{w} + \frac{1}{\cos\phi} \frac{\partial}{\partial y} (\overline{v' \theta'} . \cos\phi / \bar{\theta}_z) \qquad \ldots(15)$$

In terms of the residual mean circulation parameters $\bar{v}_R$ and $\bar{w}_R$, defined as above, the thermodynamic and continuity equations, after making some approximations, can respectively be written as

$$\bar{w}_R \cdot \frac{\partial\bar{\theta}}{\partial z} = \bar{Q} \qquad \ldots(16)$$

$$\frac{1}{\cos\phi} \cdot \frac{\partial}{\partial y} (\bar{v}_R . \cos\phi) + \frac{1}{n(M)} \frac{\partial}{\partial z} \{ n(M) . \bar{w}_R \} = 0 \qquad \ldots(17)$$

It should be noted that the above equations do not contain any eddy terms. Next, the tracer equation in

the absence of diffusion or transience, and considering the tracer as chemically inert, takes a very simple form as

$$\frac{\partial \bar{\mu}}{\partial t} + \bar{v}_R \cdot \frac{\partial \bar{\mu}}{\partial y} + \bar{w}_R \cdot \frac{\partial \bar{\mu}}{\partial z} = P - L \qquad \ldots(18)$$

The formulation in isentropic coordinates adopts the potential temperature as the vertical coordinate. The vertical velocity is proportional to the diabatic heating and the zonal mean circulation is a close approximation of the diabatic circultion. This formultion offers some conceptual advantages over the residual mean formulation for tracer modelling.

It must be emphasized that the residual and diabatic circulations are only approximate, although good approximations in the stratosphere, and some eddy transport must be included to account for the irreversible processes like transience, dissipation, etc. For instance, Holton[67] considered eddy forcing in the thermodynamic equation and Garcia and Solomon[68] considered eddy terms in both the thermodynamic and momentum equations.

4.1 Discussion on 2-D Model Results and Some Comparisons with Observations

An excellent overview of the results obtained from 2-D models and their comparison with observations as well as with themselves was compiled in the *WMO report No.* 16 (Ref. 18). The salient points are summarized here.

With regard to the simulation of long-lived tracers, the so called source gases, 2-D models fall roughly into two general classes, viz. those in which advection and diffusion play nearly equal roles (these models use relatively large eddy diffusion coefficients); and those in which advection dominates over diffusion (these models use eddy diffusion coefficients which are about an order of magnitude smaller than those used in the former models). The source gases have their sources in the troposphere and are injected into the stratosphere, mainly at the tropics, through the ascending air parcels there. As these parcels move polewards, destruction by photolysis occurs in the stratosphere and the concentrations become lower. At the poles, where the air descends, the mixing ratios are lower than those in the tropics, and the isolines descent to lower altitudes at the poles. Obviously, in models that use higher eddy diffusion coefficients, horizontal mixing is more efficient and the isolines are flatter than in those models which use smaller eddy diffusion coefficient values. The results for all the source gases obtained from different 2-D models reveal this general feature.

The main odd oxygen species in the stratosphere is ozone. The important features of the observed ozone distribution are: (i) low equatorial abundances, (ii) an increase towards high latitudes, and (iii) a strong seasonal variation at mid- and high-latitudes (50-60°), with the concentration being maximum in spring and minimum in autumn. In general, the results obtained from models using high eddy diffusion coefficient values (classical Eulerian models) underestimate the latitudinal contrast and overestimate the ozone column at equatorial latitudes. The diabatic and residual circulation models reflect the lower abundances at equatorial latitudes well. These models show larger latitudinal gradients and sometimes the calculated abundances at high latitudes are too high.

An intercomparison of models results for ozone distribution show considerable differences. These are believed to arise from the differences in the adopted values of diabatic heating rates and diffusion coefficients. The differences between results from different models are significant in the lower stratosphere, which happens to be a dynamically controlled region.

The results for the odd hydrogen species obtained from different models show morphological features which are similar. The salient features are: a broad peak in the altitude range 40-45 km, a saddle-shaped minimum near the tropopause and a steep gradient towards the winter pole. While there is an agreement between modelled results of OH with observations, the agreement is not so good in respect of HO_2 and H_2O_2. It is to be mentioned that measurements of HO_2 are rather limited. The observed deviations are, therefore, to be taken with some care. But, if these differences were to be real, they imply a problem with our understanding of the photochemistry and hence the partitioning of the HO_x family, in view of the agreement between the observations of OH and the model results.

The modelled total odd nitrogen is crucial to the ozone balance and, therefore, for the evaluation of possible future changes in ozone column. Odd nitrogen (NO_y) is a very long-lived species, and its horizontal gradient depends sensitively on the relative roles of horizontal mixing and advection, considered in the total transport. A comparison of modelled NO_y results obtained by Gray and Pyle[71] using a classical Eulerian model, with those obtained by Ko *et al.*[72] who used an advection dominated residual circulation model, demonstrates this aspect. The results of NO_y obtained by Ko *et al.*[72], showed much steeper slope in latitude than do the results of Gray and Pyle[71], as pointed out in the *WMO report No.* 16 (Ref. 18).

A comparison of altitude distributions of NO_y for tropical, mid-and high-latitudes obtained from several 2-D models shows marked differences, particularly above 40 km. This is found to be mainly attributable

to differences in the calculated NO photolysis rates (Ref. 18).

From what has been discussed above, it appears that a choice of proper transport formulation and parametrization of photolysis rates are important for improving the accuracy of modelled odd nitrogen distributions.

Odd chlorine species (Cl_y), which are important in the stratosphere, can be separated into HCl and Cl_x ($Cl + ClO + ClONO_2 + HOCl$). The species forming the Cl_x group have much shorter chemical interconversion times (a few hours), when compared to the interconversion time between HCl and Cl_x which is of the order of a day or longer as pointed out by Ko and Sze[73].

The overall distributions of the Cl_y obtained as a function of altitude and latitude from different 2-D models are similar, although some differences exist in the lower stratosphere. These differences are believed to arise from the differences in the transport schemes and the heterogeneous removal processes adopted in different models.

Acknowledgement

The authors are thankful to the University Grants Commission (UGC), New Delhi, for the financial support provided under a UGC/IMAP research project.

References

1 Crutzen P J, *Q J R Met Soc (GB)*, **96** (1970) 320.
2 Johnston H S, *Science (USA)*, **173** (1971) 517.
3 Molina M J & Rowland F S, *Nature (GB)*, **249** (1974) 810.
4 Chapman S, *Mem R Met Soc (GB)*, **3** (1930) 103.
5 Bates D R & Nicolet M, *J Geophys Res (USA)*, **55** (1950) 301.
6 Hunt B G, *J Atmos Sci (USA)*, **23** (1966) 88.
7 Ackerman M & Muller C, *Pure Appl Geophys (Switzerland)*, **106-108** (1973) 1325.
8 Ackerman M, Fontanella J C, Frimout D, Girard A, Louisnard N & Muller C, *Planet & Space Sci (GB)*, **23** (1975) 651.
9 Cicerone R J, Stolarski R S & Walters S, *Science (USA)*, **185** (1974) 1165.
10 Stolarski R S & Cicerone R J, *Can J Chem (Canada)*, **52** (1974) 1610.
11 Wofsy S C & McElroy M B, *Can J Chem (Canada)*, **52** (1974) 1582.
12 Crutzen P J, *Can J Chem (Canada)*, **52** (1974) 1569.
13 Crutzen P J, *Geophys Res Lett (USA)*, **1** (1974) 205.
14 Wofsy S C, McElroy M B & Sze N D, *Science (USA)*, **187** (1975) 535.
15 Turco R P & Whitten R C, *Atmos Environ (GB)*, **9** (1975) 1045.
16 Crutzen P J, Isaksen I S A & McAfee J R, *J Geophys Res (USA)*, **83** (1978) 345.
17 Deshpande S D & Mitra A P, *Sci Rep ISRO-IMAP-SR-11-83*, 1983.
18 *WMO Report on Global Ozone Research and Monitoring Report No. 16, (USA)*, 1986.
19 Mount G H, Rottman G J & Timothy J G, *J Geophys Res (USA)*, **85** (1980) 4271.
20 Mount G H & Rottman G J, *J Geophys Res (USA)*, **86** (1981) 9193.
21 Mount G H & Rottman G J, *J Geophys Res (USA)*, **88** (1983) 5403.
22 Mount G H & Rottman G J, *J Geophys Res (USA)*, **90** (1985) 13031.
23 Rottman G J, *Planet & Space Sci (GB)*, **31** (1983) 1001.
24 London J, Bjarnason G G & Rottman G J, *Geophys Res Lett (USA)*, **11** (1984) 54.
25 Heath D F, Repoff T P & Donnelly R F, *Nimbus-7 SBUV observations of solar UV spectral irradiance variations caused by solar rotation and active-region evolution for the period* 7 Nov. 1978-1 Nov. 1980, *NOAA-TM-ERL-ARL-129*, NOAA Air Resources Laboratory, Rockville, MD, USA, 1984, p. 78.
26 Heath D F & Schlesinger B M, *J Geophys Res (USA)*, **91** (1986) 8672.
27 Cieslik S & Nicolet M, *Planet & Space Sci (GB)*, **21** (1973) 925.
28 Lettau H, *Compendium of Meteorology* (American Meteorological Soc., New York, USA), 1951, 320.
29 Zimmerman S P & Champion K S W, *J Geophys Res (USA)*, **68** (1963) 3049.
30 Kenneshea T J & Zimmerman S P, *J Atmos Sci (USA)*, **27** (1970) 831.
31 Reed R J & German K E, *Mon Weath Rev (USA)*, **93** (1965) 313.
32 Ebel A, *J Atmos & Terr Phys (GB)*, **42** (1980) 617.
33 Wuebbles D J, *J Geophys Res (USA)*, **88** (1983) 1433.
34 Holton J R, *Hand Book for MAP*, edited by S Kato (USA), Vol. 18, 1985, Ch. 4.
35 Mahlman J D, Levy II H B & Moxim W J, *J Geophys Res (USA)*, **91** (1986) 2687.
36 Holton J R, *J Atmos Sci (USA)*, **39** (1982) 791.
37 Solomon S, *One- and Two-dimensional Photo Chemical Modelling of the Chemical Interactions in the Middle Atmosphere* 0-120 *km*, Co-operative thesis No. 62, University of California and National Centre for Atmospheric Research, USA, 1981.
38 Hays P B & Roble R G, *Planet & Space Sci (GB)*, **21** (1973) 273.
39 Noxon J F, *J Geophys Res (USA)*, **81** (1976) 1370.
40 Llewellyn E J & Witt G, *Planet & Space Sci (GB)*, **25** (1977) 165.
41 Anderson J G, *J Geophys Res (USA)*, **76** (1971) 7820.
42 Meira C G (Jr), *J Geophys Res (USA)*, **76** (1971) 202.
43 Tohmatsu T & Iwagami N, *J Geomagn & Geoelectr (Japan)*, **28** (1976) 343.
44 Acharya Y B *et al.*, *Indo-USSR Ozonesonde Intercomparison Experiment at Thumba – Part II, Sci Rep No. ISRO-IMAP-SR-24-85*, 1985.
45 Solomon S & Garcia R R, *J Geophys Res (USA)*, **89** (1984) 11633.
46 Anderson J G, *Geophys Res Lett (USA)*, **3** (1976) 165.
47 Heaps W S & McGee T J, *J Geophys Res (USA)*, **90** (1985) 7913.
48 Weinstock E M, Phillips M J & Anderson J G, *J Geophys Res (USA)*, **86** (1981) 7273.
49 Brune W H, Weinstock E M, Schwab J J, Stimpfle R M & Anderson J G, *Geophys Res Lett (USA)*, **12** (1985) 441.
50 Murcray D G, Goldman A, Murcray F H, Murcray F J & Williams W J, *Geophys Res Lett (USA)*, **6** (1979) 857.
51 Rinsland C P, Goldman A, Murcray D G, Murcray F J, Bonomo F S, Blatherwick R B, Devi V M, Smith M A H & Rinsland P L, *J Geophys Res (USA)*, **90** (1985) 7931.
52 Prabhakara C, *Mon Weath Rev (USA)*, **91** (1963) 411.
53 Newell R E, *Pure Appl Geophys (Switzerland)*, **59** (1964) 191.

54 Rao Vupputuri R K, *Mon Weath Rev US Dep Agric (USA)*, **101** (1973) 510.
55 Harwood R S & Pyle J A, *Q J R Meteorol Soc (GB)*, **101** (1975) 723.
56 Mahlman J D, *Proceedings of the Fourth Conference on Climatic Impact Assessment Programme DOT-TSC-OST-75-38*, edited by T M Hard and A J Broderick, 1975, 132.
57 Matsuno T, *Pure Appl Geophys (Switzerland)*, **118** (1980) 189.
58 Clark J H E & Rogers T G, *J Atmos Sci (USA)*, **35** (1978) 2232.
59 Plumb R A, *J Atmos Sci (USA)*, **36** (1979) 1699.
60 Danielsen E F, *J Atmos Sci (USA)*, **38** (1981) 1319.
61 Andrews D G & McIntyre M E, *J Fluid Mech (GB)*, **89** (1978) 609.
62 McIntyre M E, *Pure Appl Geophys (Switzerland)*, **118** (1980) 152.
63 Andrews D G & McIntyre M E, *J Atmos Sci (USA)*, **33** (1976) 2031.
64 Boyd J P, *J Atmos Sci (USA)*, **33** (1976) 2285.
65 Dunkerton T J, *J Atmos Sci (USA)*, **35** (1978) 2325.
66 Holton J R, *Phil Trans R Soc London A (GB)*, **296** (1980) 73.
67 Holton J R, *J Geophys Res (USA)*, **86** (1981) 11989.
68 Garcia R R & Solomon S, *J Geophys Res (USA)*, **88** (1983) 1379.
69 Mahlman J D, Andrews D G, Duetsch H U, Hartmann D L, Matsuno T, Murgatroyd R J & Noxon J F, *Hand Book for MAP*, Vol. 3, edited by C F Sechrist (Jr), USA, 1981, p. 14.
70 Tung Ka Kit, *J Atmos Sci (USA)*, **39** (1982) 2330.
71 Gray L J & Pyle J A, *Q J R Meteorol Soc (GB)*, **113** (1987) 635.
72 Ko M K W, Tung K K, Weinstein D K & Sze N D, *J Geophys Res (USA)*, **90** (1985) 2313.
73 Ko M K W & Sze N D, *J Geophys Res (USA)*, **89** (1984) 11619.